2010 American Control Conference
Marriott Waterfront, Baltimore, MD, USA
June 30-July 02, 2010

Leader follower based formation control strategies for nonholonomic mobile robots: Design, Implementation and Experimental Validation

Gayan W. Gamage, George K. I. Mann and Raymond G. Gosine

Abstract— **This paper proposes novel formation maintenance strategies for multiple nonholonomic mobile robots based on nonholonomic trajectory tracking techniques and dynamic feedback linearization. It also presents experimental results for formation stability and noise tolerance of the proposed and existing leader-follower based controllers using physical P3AT robots. The research focusses only on the problem of formation maintenance by multiple nonholonomic mobile robots. Two types of formation maintenance controllers are developed by transforming the follower robot's motion in to separate trajectory tracking tasks and then by applying existing nonholonomic trajectory tracking techniques. A third controller is developed through the use of dynamic feedback linearization. The proposed systems are implemented in physical P3AT type mobile robots and real-world experimental results are shown to compare the formation accuracy and the stability of these controllers.**

Index Terms - multi-robot formation control, nonholonomic mobile robots, trajectory tracking

I. INTRODUCTION

Formation control of multiple robots is inspired partly by the necessacity of the nature of the tasks and partly by the formation behavior of schools of fishes or flocks of birds [1], where multiple agents combine their senses for efficient food finding or combining their thrust in the liquid or air to move forward as one pack. It's usage has been explored for search and rescue missions [2],[3], reconnaissance and patrols [4], satellite control and automated highways [5]. The basic formation control problem consists of maintaining desired geometric formations of varied shapes and sizes e.g.: triangular, line or column. Many types of control techniques have been proposed to tackle the formation maintenance problem. Some techniques involve leader-follower formation control [6],[7],[8], virtual structure approach [9], behavior-based formation control [1] and consensus based formation control [10]. Although centralized, the leader-follower based formation control strategies have been widely exploited for formation control applications owing to their flexibility, simple operation, scalability and lesser computational demand. The research problem addressed in this paper revolves around the leader-follower formation control paradigm.

1) Problem I: Nonlinear control laws for formation control of nonholonomic mobile robots: The formation control can be thought of as a combination of trajectory tracking and posture stabilization [11] of nonholonomic mobile robots. There exists a number of nonlinear time invariant, time varying or discontinuous [12],[11],[13] control techniques proposed and implemented for posture stabilization and trajectory tracking of nonholonomic mobile robots. These numerous nonlinear control techniques have not been exploited for formation control of multiple nonholonomic mobile robots. The extensive literature review also suggests that, out of all the existing leader-follower based control theoretic approaches, the $l-\psi$ controller proposed by Desai et al.[8] through static feedback linearization has more flexibility and scalability for formation control applications. But since this controllers stabilize not the follower robot's origins* (origin refers to the origin of the robot coordinate system where the calculated robot pose is taken through it's odometry readings), but an offset from their origins to desired geometric poses leads to: *1.)* not fulfilling the real objectives of formation control, which is to stabilize the origins of the robot platform (origin of the follower robot coordinate system) to desired formation locations *2.)* The controller may exhibit some form of instability under noisier inputs.

2) Problem II: Comparative study of Leader-follower based control theoretic approaches: The lack of a substantial comparison of different leader-follower based formation control approaches in terms of their stability, rate of convergence and noise tolerance is identified as a potential issue. It is also identified that the real world implementation problems related to platform dynamics, wheel slippage, noises in observation etc. have also not been sufficiently evaluated for the proposed leader-follower based formation controllers through real world experiments.

The key contribution of this paper can be listed as, *1.)* development of trajectory tracking type formation maintenance controllers and a dynamic feedback linearized formation maintenance controller. *2.)* comparison of trajectory tracking, static feedback linearized and dynamic feedback linearized formation maintenance controllers in terms of formation accuracy, noise tolerance, smoothness of control inputs using P3AT mobile robots.

II. LEADER-FOLLOWER BASED FORMATION MAINTENANCE CONTROLLERS

This research proposes three types of formation maintenance controllers for the nonholonomic unicycle robots. Two of such controllers are developed through virtual robot path tracking techniques 1.) based on the approximate linearization of the unicycle dynamics described in [11], 2.)

This research is supported by the Natural Sciences and Engineering Research Council of Canada (NSERC) and Memorial University of Newfoundland, Canada

G. Gamage, G. Mann and R. Gosine are with Memorial University, Canada. {gayan,gmann,rgosine}@engr.mun.ca

based on a Lyaponov-based nonlinear time varying design described in [12]. The third controller is developed through dynamic feedback linearization. These three controllers will be compared for formation stability between themselves and also with a fourth leader-follower based static feedback linearized formation controller developed in [8]. The real world experimental validation of the proposed and existing control schemas are carried out in P3AT mobile robots. The kinematics of the P3AT mobile robots can be described by the unicycle dynamics given as,

$$\dot{x} = v\cos\theta, \quad \dot{y} = v\sin\theta, \quad \dot{\theta} = \omega \tag{1}$$

Where $\mathbf{x} = (x, y, \theta) \in SE(2)$ and v and ω are the linear and angular velocities respectively. P3AT is a four wheel differential drive mobile robot with $50cm$ x $49cm$ x $26cm$ aluminum body with $21.5cm$ diameter drive wheels. The P3AT robot also has saturation levels of the linear and angular velocities and linear and angular accelerations.

$$\begin{aligned} |v| \le v_{max} &= 0.6ms^{-1}, & |\omega| \le \omega_{max} &= 0.75rads^{-1} \\ |a| \le a_{max} &= 0.3ms^{-2}, & |\alpha| \le \alpha_{max} &= 0.8rads^{-2} \end{aligned}$$

a and α are the linear and angular accelerations respectively. v_{max}, ω_{max} are the absolute maximum linear and angular velocities of the robot while a_{max} and α_{max} are the absolute maximum linear and angular accelerations of the robot respectively. In order to preserve the curvature radius originated from v and ω, a velocity scaling is needed as follows, If the scaled down linear and angular velocities are v_s and ω_s respectively, we have:

$$\begin{aligned} \Lambda = max\{|v|/v_{max}, \quad |\omega|/\omega_{max}, \quad 1\} \\ v_s = sign(v)v_{max}, \ \omega_s = \omega/\Lambda \ when\ (\Lambda == |v|/v_{max}) \\ v_s = v/\Lambda, \ \omega_s = sign(\omega)\omega_{max} \ when\ (\Lambda == |\omega|/\omega_{max}) \\ v_s = v, \ \omega_s = \omega \ when\ (\Lambda == 1) \end{aligned}$$

III. Virtual Robot Tracking Based Formation Controllers

The nonholonomic motion of the leader-robot results in a path, which can be approximated through an accumulation of straight and circular path segments [14]. The motion of any point fixed in an offset to the origin of the leader robot coordinate system results in a nonholonomic motion. In leader-follower based formation control also, the desired poses of followers can be thought of as fixed in offsets to the origin of the leader-robot coordinate system at any given time. These fixed points mimic virtual robots which the actual followers must track. Tracking such virtual robot paths and their desired velocities require a combination of a nominal feed forward command with a feedback action on the error [15]. Feed forward command generation involves calculating the pose of the virtual robot and it's linear and angular velocities to which the actual designated follower must reach to.

A. *Feedforward* Command Generation

Assuming that the leader robot's pose at time t is $[x_t \quad y_t \quad \theta_t]^T$ and the velocities being $[v_t \quad \omega_t]^T$, The desired position for the follower can be described as located in an offset of o_x units and o_y units from the origin to X and Y directions respectively in the leader robot coordinate system. $(x_t^f, y_t^f, \theta_t^f)$ is the desired pose for a follower robot in the

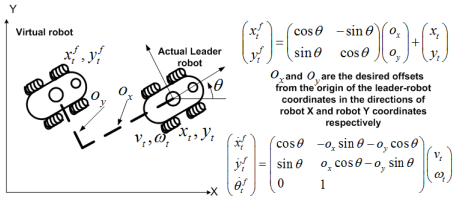

Fig. 1. Virtual robot representation for tracking based formation control

Euclidean $SE(2)$ coordinate system. E.q.2 is taken from Fig.1.

$$\begin{pmatrix} \dot{x}_t^f \\ \dot{y}_t^f \\ \dot{\theta}_t^f \end{pmatrix} = \begin{pmatrix} \cos\theta_t & -o_x\sin\theta_t - o_y\cos\theta_t \\ \sin\theta_t & o_x\cos\theta_t - o_y\sin\theta_t \\ 0 & 1 \end{pmatrix} \begin{pmatrix} v_t \\ \omega_t \end{pmatrix} \tag{2}$$

The feed-forward command generation of unicycle robots involve generating desired poses $(x_t^f, y_t^f, \theta_t^f)$ and desired velocities (v_t^f, ω_t^f) at a given time t. The desired poses can be easily taken as shown in Fig.1. The desired linear and angular velocities are taken as in [15], given by,

$$v_t^f = \pm\sqrt{\dot{x}_t^f + \dot{y}_t^f} \quad and \quad \omega_t^f = \frac{\ddot{y}_t^f \dot{x}_t^f - \ddot{x}_t^f \dot{y}_t^f}{(\dot{x}_t^f)^2 + (\dot{y}_t^f)^2} \tag{3}$$

The ω_t^f is derived through defining θ_t^f as;

$$\theta_t^f = atan2(\dot{y}_t^f, \dot{x}_t^f) + k\pi \qquad k = 0, 1 \tag{4}$$

$k = 0$ for forward motion and $k = 1$ for backward motion respectively. it is also proved below that the definition of ω_t^f in e.q.3 can be approximated to the actual angular velocity of the leader robot: ω_t.

proof: Through differentiation of $\theta_t^f = atan2(\dot{y}_t^f, \dot{x}_t^f) + k\pi$ of e.q.4, one gets,

$$\omega_t^f = \frac{\ddot{y}_t^f \dot{x}_t^f - \ddot{x}_t^f \dot{y}_t^f}{(\dot{x}_t^f)^2 + (\dot{y}_t^f)^2} \tag{5}$$

Assuming o_x and o_y are constants with $\dot{v}_t$ and $\dot{\omega}_t$ both being zero, substitution of the values of e.q.2 and it's differentiated values of $\dot{x}_t^f, \ddot{y}_t^f, \dot{x}_t^f$ and $\dot{y}_t^f$ in e.q.5 results in,

$$\omega_t^f = \omega_t \frac{((o_x^2 + o_y^2)\omega_t^2 - 2o_y v_t \omega_t + v_t^2)}{((o_x^2 + o_y^2)\omega_t^2 - 2o_y v_t \omega_t + v_t^2)} = \omega_t \quad , v_t \neq 0 \tag{6}$$

Note that ω_t^f is not defined when $v_t = 0$. In order to overcome this discontinuity at $v_t = 0$, it is proposed that the follower may switch to a posture stabilization control routine [15] at $v_t = 0$, to move to the desired pose. Hence the feed forward commands developed are,

$$v_t^f = \pm\sqrt{\dot{x}_t^f + \dot{y}_t^f} \quad and \quad \omega_t^f = \omega_t \tag{7}$$

Trajectory tracking needs to combine the feed forward commands generated in this section with an action on the feedback error. Two types of controllers which achieve such an objective are described below.

B. Approximate Linearization based formation controller

If the state tracking error is defined as in [13],

$$\begin{pmatrix} e_1 \\ e_2 \\ e_3 \end{pmatrix} = \begin{pmatrix} \cos\theta_t^s & \sin\theta_t^s & 0 \\ -\sin\theta_t^s & \cos\theta_t^s & 0 \\ 0 & 0 & 1 \end{pmatrix} \begin{pmatrix} x_t^f - x_t^s \\ y_t^f - y_t^s \\ \theta_t^f - \theta_t^s \end{pmatrix} \quad (8)$$

Where $[x_t^f, y_t^f, \theta_t^f]$ is the desired pose and $[x_t^s, y_t^s, \theta_t^s]$ is the actual follower pose at time t in the Euclidean $SE(2)$ coordinate system. The current linear and angular velocity commands (v_t^s, ω_t^s respectively) of the follower are subjected to a nonlinear transformation where the resulting newer velocity commands $[v_t^n \ \omega_t^n]$ of the follower have the following relationship,

$$\begin{pmatrix} v_t^s \\ \omega_t^s \end{pmatrix} = \begin{pmatrix} v_t^f \cos e_3 - v_t^n \\ \omega_t^f - \omega_t^n \end{pmatrix} \quad (9)$$

Then the error dynamics become,

$$\dot{e} = \begin{pmatrix} 0 & \omega_t^f & 0 \\ -\omega_t^f & 0 & 0 \\ 0 & 0 & 0 \end{pmatrix} e + \begin{pmatrix} 0 \\ \sin e_3 \\ 0 \end{pmatrix} v_t^f + \begin{pmatrix} 1 & 0 \\ 0 & 0 \\ 0 & 1 \end{pmatrix} \begin{pmatrix} v_t^n \\ \omega_t^n \end{pmatrix} \quad (10)$$

Here $e = [e_1 \quad e_2 \quad e_3]^T$. Through linearizing e.q.10 around the reference trajectory one obtains a *linear time varying system*. If a linear feedback law is defined as:

$$\begin{pmatrix} v_t^n \\ \omega_t^n \end{pmatrix} = \begin{pmatrix} -k_1 e_1 \\ -k_2 sign(v_t^f) e_2 - k_3 e_3 \end{pmatrix} \quad (11)$$

Where the choice of gains is (see [13]), $k_1 = k_3 = 2c_1\sqrt{(v_t^f)^2 + (\omega_t^f)^2}$, $k_2 = c_2 \mid v_t^f \mid$ where $c_1 \in (0,1)$ and $c_2 > 0$, one can substitute the controls of e.q.11 to the linearized system around the desired trajectory of e.q.10 to obtain,

$$\begin{aligned} v_t^s &= v_t^f \cos(\theta_t^f - \theta_t^s) + k_1((x_t^f - x_t^s)\cos\theta_t^s + (y_t^f - y_t^s)\sin\theta_t^s) \\ \omega_t^s &= \omega_t^f + k_2 sign(v_t^f)((y_t^f - y_t^s)\cos\theta_t^s - (x_t^f - x_t^s)\sin\theta_t^s) + k_3(\theta_t^f - \theta_t^s) \end{aligned} \quad (12)$$

$(x_t^f, y_t^f, \theta_t^f)$ is the desired pose and $(x_t^s, y_t^s, \theta_t^s)$ is the current follower pose in Euclidean $SE(2)$ coordinate system at time t. (v_t^f, ω_t^f) is the desired velocity at time t and (v_t^s, ω_t^s) is the follower robot velocity input at time t.

1) Experimental Results: Three P3AT mobile robots were used, two as followers and another as the leader robot. The gains of the followers were taken as $c_1 = 0.9$ and $c_2 = 15$. The experiments involved driving two of the P3AT followers for four different velocity courses of the leader robot as given below. Norm of the formation errors and the quality of the follower's driving (velocity) inputs were recorded for comparison criteria.

- leader moves with constant velocities (v_l^c, ω_l^c).
- changing angular velocities of the leader (v_l^c, ω_l^d) while keeping the linear velocity a constant.
- constant angular velocity with a changing linear velocity (v_l^d, ω_l^c).
- both linear and angular velocities are changing (v_l^d, ω_l^d)..

The formation geometry described above (see Fig.1), in terms of offsets of o_x and o_y in the respective X and Y leader robot coordinate system from it's origin is converted to a new polar geometric system (see Fig.2) for comparison ease,

$$\begin{aligned} d_{ls} &= \sqrt{(x_l - x_s)^2 + (y_l - y_s)^2} \\ \beta_{ls} &= -\theta_l + \pi + atan2(y_l - y_s, x_l - x_s) \\ \theta_{ls} &= \theta_l - \theta_s \end{aligned} \quad (13)$$

subscript l stands for the leader and s stands for the follower. (x_l, y_l, θ_l) is the pose of the leader while (x_s, y_s, θ_s) is the pose of the follower in the Euclidean $SE(2)$ coordinate system. Hence the formation errors can be described as

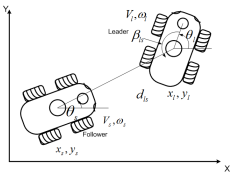

Fig. 2. Formation geometry in the new coordinates system

$e_d = d^d - d_{ls}, e_\beta = \beta^d - \beta_{ls}$ and $e_\theta = \theta^d - \theta_{ls}$. (d^d, β^d, θ^d) are the desired and $(d_{ls}, \beta_{ls}, \theta_{ls})$ are the current values for the formation variables. The resulting formation errors for an example velocity course by the application of approximate linearization based formation control are depicted in Fig.3. The follower-1's desired formation geometry is $(d_{ls}^{desired} = 1\text{m}, \beta_{ls}^{desired} = \frac{\pi}{2} rads, \theta_{ls} = 0 rads)$ and the other depicted follower-2's desired formation variables values are $(d_{ls}^{desired} = \sqrt{8}\text{m}, \beta_{ls}^{desired} = \frac{-2\pi}{3} rads, \theta_{ls} = 0 rads)$. It is observed that the distance-d_{ls} and the bearing-β_{ls} errors converge almost to zero in both followers, while the relative orientation difference-θ_{ls} error stays small: bounded around zero. When the desired bearing is $\pm\frac{\pi}{2}$, the relative orientation error θ_{ls} goes almost around zero while for other desired bearing values, the θ_{ls} error stays bounded around zero. The velocity profiles for these two followers are depicted in Fig.4.

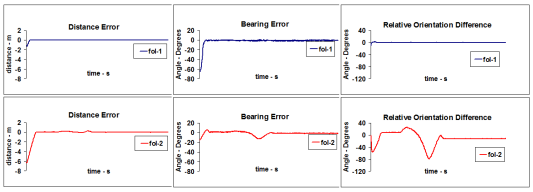

Fig. 3. Formation errors for two follower robots with approximate linearization based controller

C. Lyapunov function based nonlinear formation controller:

For the same error dynamics given in e.q.10, If the linear and angular velocity controls are defined as in [12],

$$\begin{pmatrix} v_t^n \\ \omega_t^n \end{pmatrix} = \begin{pmatrix} -k_1(v_t^f, \omega_t^f)e_1 \\ -\bar{k}_2 v_t^f \frac{\sin e_3}{e_3} e_2 - k_3(v_t^f, \omega_t^f)e_3 \end{pmatrix} \quad (14)$$

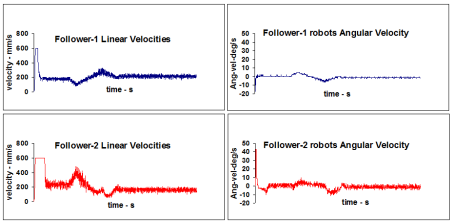

Fig. 4. Linear and angular velocities for the two follower robots with approximate linearization based controller

(v_t^s, ω_t^s) are the current linear and angular velocities of the follower robot. (v_t^f, ω_t^f) are the desired linear and angular velocities. $\bar{k}_2 > 0$ while $k_1(v_t^f, \omega_t^f)$ and $k_3(v_t^f, \omega_t^f)$ being continuous positive gain functions. (e_1, e_2, e_3) are defined as in e.q.8. (v_t^n, ω_t^n) are the the new linear and angular velocity inputs to the followers. Equation.14 becomes a controller based on a Lyapunov function of,

$$V = \frac{\bar{k}_2}{2}(e_1^2 + e_2^2) + \frac{e_3^2}{2} \text{ with } \dot{V} = -k_1\bar{k}_2 e_1^2 - k_3 e_3^2 \leq 0$$

When v_t^f, ω_t^f and its derivatives are bounded and if $v_t^f \nrightarrow 0$ and $\omega_t^f \nrightarrow 0$ as $t \rightarrow \infty$, the above controls in e.q.14 globally asymptotically stabilizes the origin $e \equiv 0$ [12]. Using similar choices for the gains as in the approximate linearized formation controller, $k_1 = k_3 = 2c_1\sqrt{(v_t^f)^2 + (\omega_t^f)^2}$ where $c_1 \in (0,1)$ and $k_2 = b > 0$, the application of the controls of e.q.14 to the error dynamics of e.q.10 results in,

$$\begin{aligned} v_t^s &= v_t^f \cos(\theta_t^f - \theta_t^s) + k_1((x_t^f - x_t^s)\cos\theta_t^s + (y_t^f - y_t^s)\sin\theta_t^s) \\ \omega_t^s &= \omega_t^f + k_2 v_t^f \frac{\sin(\theta_t^f - \theta_t^s)}{\theta_t^f - \theta_t^s}((y_t^f - y_t^s)\cos\theta_t^s - (x_t^f - x_t^s)\sin\theta_t^s) + k_3(\theta_t^f - \theta_t^s) \end{aligned} \quad (15)$$

$(x_t^f, y_t^f, \theta_t^f)$ is the desired pose and $(x_t^s, y_t^s, \theta_t^s)$ is the current follower pose in Euclidean $SE(2)$ coordinate system at time t. (v_t^f, ω_t^f) is the desired velocity at time t and (v_t^s, ω_t^s) is the follower robot velocity inputs at time t.

1) Experimental Results: The gains and the desired geometric poses are chosen as similar to the above experiment. This behavior of the controller is similar to the "Approximate

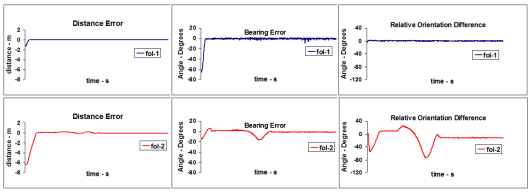

Fig. 5. Formation errors for two follower robots with Lyapunov based nonlinear control

linearization based formation controller" above. Here also the relative orientation error stays bounded for all the bearing values except for $\pm\frac{\pi}{2}$ where the error goes to zero.

IV. Static and Dynamic Feedback Linearized Formation Controllers

This section presents two other formation controllers whose error coordinates are transformed to the new coordinate system as shown in Fig.2. One such controller is developed in this research through dynamic feedback linearization while a fourth static feedback linearized formation controller with the new error coordinates, developed in [8] is used for comparison purposes. Differentiation of the formation variables of e.q.13 results in,

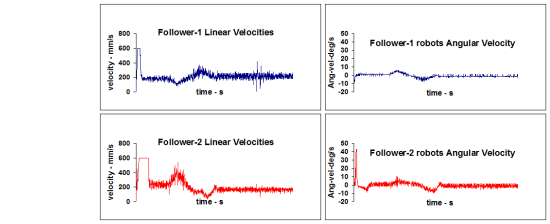

Fig. 6. Velocity profiles of the two follower robots with Lyapunov based nonlinear control

$$\begin{pmatrix} \dot{d}_{ls} \\ \dot{\beta}_{ls} \\ \dot{\theta}_{ls} \end{pmatrix} = \begin{pmatrix} \cos\gamma_{ls} & 0 \\ \frac{-\sin\gamma_{ls}}{d_{ls}} & 0 \\ 0 & -1 \end{pmatrix} \begin{pmatrix} v_s \\ \omega_s \end{pmatrix} + \begin{pmatrix} -\cos\beta_{ls} & 0 \\ \frac{\sin\beta_{ls}}{d_{ls}} & -1 \\ 0 & 1 \end{pmatrix} \begin{pmatrix} v_l \\ \omega_l \end{pmatrix} \quad (16)$$

where $\theta_{ls} = \theta_l - \theta_s$ is the relative orientation between the leader and follower. $\gamma_{ls} = \theta_{ls} + \beta_{ls}$, while $u_l = [v_l \quad \omega_l]$ is the exogenous input by the leader robot to the system. $u_s = [v_s \quad \omega_s]$ is the follower's driving inputs. The decoupling matrix (decouples control variables from state variables) in this context is singular.

A. Static feedback linearized formation controller

To overcome the singularity of e.q.16, [8] proposes a static feedback linearization by shifting the current output state vector to an offset from the origin of the robot coordinate system. The control input to the followers are given by,

$$\mathbf{u_s} = G_1^{-1}(k(z_{ls}^d - z_{ls}) - F_1\mathbf{u_l}) \quad (17)$$

$$G_1 = \begin{pmatrix} \cos\gamma_{ls}^n & p_x\sin\gamma_{ls}^n \\ \frac{-\sin\gamma_{ls}^n}{d_{ls}^n} & \frac{p_x\cos\gamma_{ls}^n}{d_{ls}^n} \end{pmatrix}, F_1 = \begin{pmatrix} -\cos\beta_{ls}^n & 0 \\ \frac{\sin\beta_{ls}^n}{d_{ls}^n} & -1 \end{pmatrix}$$

where $\gamma_{ls}^n = \theta_{ls}^n + \beta_{ls}^n$ and p_x is the offset along the X coordinate of the robot described earlier. $z_{ls} = [d_{ls}^n \quad \beta_{ls}^n]^T$ is the system output with the above offset p_x and $\theta_{ls}^n = \theta_l - \theta_s$ is the new relative orientation between the leader and follower. $u_l = [v_l \quad \omega_l]$ is the exogenous input by the leader robot to the system while $u_s = [v_s \quad \omega_s]$ is the follower's driving inputs. $k = [k_1 \quad k_2]^T > 0$ are the controller gains, while $z_{ls}^d = [d_{ls}^d \quad \beta_{ls}^d]^T$ are the desired relative distance and bearing of the follower robot from the leader robot.

1) Simulation Results: For the same experiment run above,the formation errors for the two followers are shown in Fig.7. The velocity profiles for these two followers with nonlinear static feedback linearization are depicted in Fig.8. As can be seen from Fig.7, relative orientation error stays bounded as proved in [8]. Angular velocity of the follower-2 seems quite noisy when compared to the angular velocities, generated from previous controllers for the same follower.

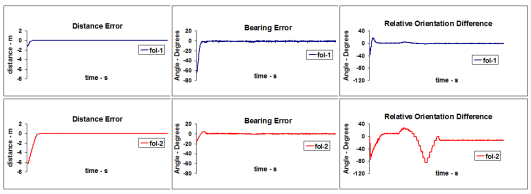

Fig. 7. Formation errors for two follower robots with static feedback linearized control

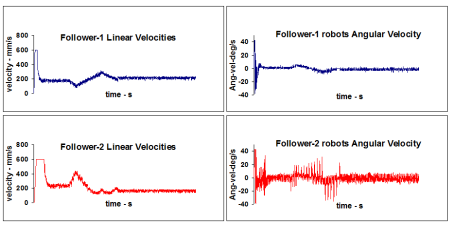

Fig. 8. Velocity profiles for the two followers with static feedback linearized control

B. Dynamic feedback linearized formation controller

The singularity of the decoupling matrix of e.q.16, is removed through the dynamic extension [16],[17],[18] such that the linear velocity v_s of the follower robot is taken as a dynamic state while the first integrator of v_s is taken as a control variable for the follower along with ω_s.

$$\xi_s = v_s, \quad \dot{\xi}_s = a_s \tag{18}$$

a_s is the linear acceleration of the follower and ξ_s is the dynamic extension to v_s. Substituting the new variables to e.q.16 and differentiating results in,

$$\ddot{z}_{ls} = G_2(z_{ls}, \theta_{ls}, \xi_s)\hat{\mathbf{u_s}} + F_2(z_{ls}, \theta_{ls}, \xi_s)\hat{\mathbf{u_l}} + \mathbf{L} \tag{19}$$

$\theta_{ls} = \theta_l - \theta_s$ and $z_{ls} = [d_{ls} \quad \beta_{ls}]^T$ is the system output and $\hat{u_l} = [a_l \quad \omega_l]$ is the exogenous input by the leader robot where a_l is the linear acceleration of the leader and ω_l is the angular velocity. $\hat{u_s} = [a_s \quad \omega_s]$ is the follower's driving inputs and a_s is it's linear acceleration while ω_s is the angular velocity. G_2, F_2 and $\mathbf{L}$ are given as,

$$G_2 = \begin{pmatrix} \cos\gamma_{ls} & \xi_s \sin\gamma_{ls} \\ \frac{-\sin\gamma_{ls}}{d_{ls}} & \frac{\xi_s \cos\gamma_{ls}}{d_{ls}} \end{pmatrix}, F_2 = \begin{pmatrix} -\cos\beta_{ls} & -\xi_s \sin\gamma_{ls} \\ \frac{\sin\beta_{ls}}{d_{ls}} & \frac{-\xi_s \cos\gamma_{ls}}{d_{ls}} \end{pmatrix}$$

$$\mathbf{L} = \begin{pmatrix} v_l\dot{\beta}_{ls}\sin\beta_{ls} - \xi_s\dot{\beta}_{ls}\sin\gamma_{ls} \\ \frac{\xi_s\dot{d}_{ls}\sin\gamma_{ls}}{d_{ls}^2} + \frac{v_l\dot{\beta}_{ls}\cos\beta_{ls}}{d_{ls}} - \frac{v_l\dot{d}_{ls}\sin\beta_{ls}}{d_{ls}^2} - \frac{\xi_s\dot{\beta}_{ls}\cos\gamma_{ls}}{d_{ls}} - \dot{\omega}_l \end{pmatrix}$$

In spite of the dynamic extension there exists a potential singularity, when $\xi_s = v_s = 0$. It is a structural singularity to nonholonomic unicycle type mobile robots[15]. In order to overcome this singularity, this research uses only a naive approach that resets the state of ξ_s, once the velocity of the axel falls below a lower threshold. This can be accomplished through imposing a constraint for the followers as : the linear velocity of the follower $v_s > ||v_s^{lower}||$ where v_s^{lower} is the lower threshold, a smaller positive value. If v_s falls in between $-v_s^{lower}$ and $+v_s^{lower}$ from any feedback controls, then v_s is reset to $-v_s^{lower}$ or $+v_s^{lower}$ depending on which side (negative or positive) the follower velocity decreased from. Thus it results in a bounded velocity input with isolated discontinuities with respect to time. Through nonlinear dynamic feedback linearization of e.q.19 one gets,

$$\hat{\mathbf{u_s}} = G_2^{-1}(C - F_2\hat{\mathbf{u_l}} - \mathbf{L}) \tag{20}$$

Here C is given by $C = [c_1 \quad c_2]^T$.

$$\ddot{z}_{ls} = \begin{pmatrix} c_1 \\ c_2 \end{pmatrix} = \begin{pmatrix} \ddot{d}_{ls}^d + k_1(\dot{d}_{ls}^d - \dot{d}_{ls}) + k_2(d_{ls}^d - d_{ls}) \\ \ddot{\beta}_{ls}^d + k_1(\dot{\beta}_{ls}^d - \dot{\beta}_{ls}) + k_2(\beta_{ls}^d - \beta_{ls}) \end{pmatrix} \tag{21}$$

$z_{ls}^d = [d_{ls}^d \quad \beta_{ls}^d]^T$ are the desired relative distance and bearing of the follower robot from the leader robot. (k_1, k_2, k_3, k_4) are controller gains. By applying the inputs of e.q.20 to the closed loop system resulting from e.q.21, the outputs $[d_{ls} \quad \beta_{ls}]$ exponentially converges to the desired values. Hence in order to prove the given system is stable, it is sufficient show that the orientation error θ_{ls} remains bounded as $t \to \infty$. By assuming that, leader robots $v_l > 0$ and $\| \omega_l \| \leq W_{max}$ and the follower $v_{max} \geq v_s > v_s^{lower}$, $\| a_s \| \leq a_{max}$ and $\| \omega_s \| \leq W_{max}$, stability theory of perturbed systems [17], can be used to prove,

$$\| \theta_{ls} \| \leq \delta \text{ for small } \delta \geq 0 \text{ as } t \to \infty.$$

1) Experimental Results: The same experiment is performed for this controller with gains of: $k_i = 0.9$ for $i = (1, .., 4)$. The formation errors over time for the two followers are shown in Fig.9. The initial starting velocities of both follower robots are 0.01m/s. Again it is seen that the relative

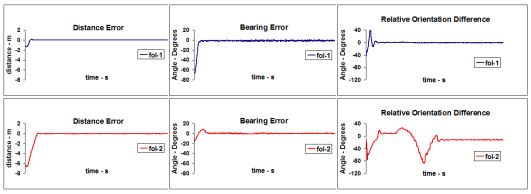

Fig. 9. Formation errors for two follower robots with dynamic feedback linearized control

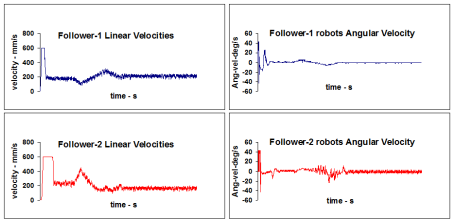

Fig. 10. Velocity profiles for the two followers with dynamic feedback linearized control

orientation error stays bounded. It is also observed that the linear and angular velocities are much smoother than the command velocities obtained by the previously experimented controllers.

V. Formation Controller Comparison

Formation errors and the quality of the command inputs of the four controllers described above, are considered for

comparison. The same set of experiments with different leader velocity profiles are performed for the different formation controllers explained above. The formation controllers developed above are listed as controller 1 to 4.

- controller 1 - Approximate linearized trajectory tracking type formation controller
- controller 2 - Lyapunov based trajectory tracking type formation controller
- controller 3 - Static feedback linearized $d-\beta$ type formation controller
- controller 4 - Dynamic feedback linearized $d-\beta$ type formation controller

The resulting formation RMS errors per follower robot per unit time is given in Table I. Individual $d_{ls}^{error}, \beta_{ls}^{error}, \theta_{ls}^{error}$ as well as holistic $\frac{d_{ls}^{error}+\beta_{ls}^{error}+\theta_{ls}^{error}}{3}$ errors are given for each velocity profile of the leader. Lastly the average individual and holistic RMS error component are given for each controller.

RMS errors	d_{ls}^{error}	β_{ls}^{error}	θ_{ls}^{error}	holistic error
velocity profile-1				
controller 1	0.0533	2.5741	18.3964	7.0080
controller 2	0.0718	3.2726	**18.2408**	7.1951
controller 3	**0.0128**	**0.8470**	19.0622	6.6407
controller 4	0.0166	1.0526	18.6247	**6.5646**
velocity profile-2				
controller 1	0.0423	2.0728	**5.3498**	2.4883
controller 2	0.5493	3.8823	8.1171	4.1829
controller 3	**0.0284**	**1.4150**	5.5565	**2.3333**
controller 4	0.0361	1.8062	5.3780	2.4068
velocity profile-3				
controller 1	0.3345	10.3393	24.1732	11.6157
controller 2	**0.3100**	12.0413	**22.1300**	**11.4938**
controller 3	0.6143	**8.9711**	24.9390	11.5081
controller 4	0.8511	10.3688	24.7626	11.9942
Average Error for all the above velocity profiles				
controller 1	**0.1434**	4.9954	**15.9731**	7.0373
controller 2	0.3104	6.3987	16.1626	7.6240
controller 3	0.2185	**3.7444**	16.5192	**6.8274**
controller 4	0.3013	4.4092	16.2551	6.9885

TABLE I

RMS FORMATION ERROR VALUES FOR THE DIFFERENT FORMATION CONTROLLERS DEVELOPED ABOVE

VI. CONCLUSION

From these results it's sufficient to conclude that the static feedback linearized controller outperforms it's counterparts with a narrow margin. It minimizes β_{ls}^{error} to a much lesser value than others but suffers from a high θ_{ls}^{error} value. Another flaw of this controller is that the given formation control law does not stabilize the origin* (considered as the origin of the robot coordinate system of the robot where the robot pose is calculated from it's odometry readings) of the follower robot, instead an offset point from the origin to desired formation values. Thus the comparison of these values may be somewhat controversial. On the other hand, both approximate linearized and Lyapunov based nonlinear trajectory tracking type controllers keep the θ_{ls}^{error} at a possible minimum. The approximate linearized formation controller also tries to keeps d_{ls}^{error} at much more lower values throughout the experiment than the others. The Lyapunov based nonlinear formation controller has shown better performance with varying v_l and ω_l. The dynamic feedback linearized controller is next best to the static feedback linearized controller. Observing the velocity command inputs of the followers, it can be concluded that both 1.) approximate feedback linearized, and 2.)nonlinear Lyapunov based controllers exerts much oscillation in their respective linear velocities but quite stable in rendering the angular velocities. Static and dynamic feedback linearized controllers renderers a much smoother linear velocity profile for all the followers. But the static feedback linearized controller has more noisy angular velocity profile (Highly oscillating), where as the dynamic feedback linearized controller has a very smooth angular velocity profile across all followers, more smoother than it's counterparts.

REFERENCES

[1] T. Balch and R. Arkin, "Behaviour-based formation control for multi-robot systems," *IEEE T. on Robotics and Automation*, vol. 14, no. 6, pp. 926–939, August 1998.

[2] R. Murphy., "Human-robot interaction in rescue robotics," *IEEE Transactions on Systems, Man and Cybernetics*, vol. 34, no. 2, p. 138153, May 2004.

[3] I. R. Nourbakhsh, K. Sycara, M. Koes, M. Yong, M. Lewis, and S. Burion, "Human-robot teaming for search and rescue," *IEEE Pervasive Computing*, vol. 4, no. 1, pp. 72–78, March 2005.

[4] D. Voth, "A new generation of military robots," *IEEE Intelligent Systems*, vol. 19, no. 4, p. 23, August 2004.

[5] P. Varaiya, "Smart cars on smart roads: problems of control," *IEEE Transactions on Automatic Control*, vol. 38, no. 2, p. 195207, February 1993.

[6] A. Das, J. P. Ostrowski, and V. Kumar, "Modeling and control of formations of nonholonomic mobile robots," *IEEE T. on Robotics and Automation*, vol. 17, no. 6, pp. 905–908, December 2001.

[7] O. A. Orqueda and R. Fierro, "Visual tracking of mobile robots in formation," *American Control Conference*, 2007.

[8] A. Das, R. Fierro, V. Kumar, J. Ostrowski, J. Spletzerm, and C. Taylor, "A vision-based formation control framework," *IEEE T. on Robotics and Automation*, vol. 18, no. 5, pp. 813–825, October 2002.

[9] K. Tan and M. Lewis, "Virtual structures for high precision cooperative mobile robot control," *Auton. Robots*, vol. 4, pp. 387–403, Oct 1997.

[10] W. Ren, "Consensus strategies for cooperative control of vehicle formations," *IEEE Control Theory Appl*, vol. 1, no. 2, pp. 505–512, April 2007.

[11] A. D. Luca, G.Oriolo, and C.Samson, "Feedback control of a non-holonomic car-like robot," *Robot Motion Planning and Control*, 1998.

[12] C. Samson, "Time-varying feedback stabilization of car-like wheeled mobile robots," *International Journal of Robotics Research*, vol. 12, no. 1, pp. 55–64, 1993.

[13] C. de wit, H. Khennouf, C. Samson, and O. Sordalen, *Nonlinear Control Design for mobile Robots*. Y.F Zheng Ed. Singapore: World Scientific, 1993.

[14] D. Fox, W. Burgard, and S. Thrun, "A dynamic window approach to collision avoidance," *IEEE Robotics and Automation Magazine*, pp. 1070–9932, March 1997.

[15] G. Oriolo, A. D. Luca, and M. Vendittelli, "Wmr control via dynamic feedback linearization: Design, implementation and experimental validation," *IEEE Trans. Contr. Syst. Technol.*, vol. 10, no. 6, pp. 835–852, 2002.

[16] A. Isidori, *Nonlinear Control Systems*. Springer, 1989.

[17] H. K. Khalil, *Nonlinear Systems*. Prentice Hall, 1996.

[18] R. Brockett, R. Millmann, and H. Sussmann, *Differential Geometric Control Theory*. Birkhauser, 1983.